

Mechanism of scaphoid waist fracture: finite element analysis

John Ashutosh Santoshi¹ , Prateek Behera¹,
Ravi Kumar Dwivedi² and Ayush Srivastav²

Journal of Hand Surgery

(European Volume)

0(0) 1–9

© The Author(s) 2022

Article reuse guidelines:

sagepub.com/journals-permissions

DOI: 10.1177/17531934221145516

journals.sagepub.com/home/jhs



Abstract

The mechanism of scaphoid waist fracture is not completely understood. We used finite element analysis to study the formation of scaphoid waist fractures. Clinical computed tomography scans of 12 wrists were used to create models for finite element analysis. The points of application of load were at different sites along the scaphotrapezotrapezoid joint distally, and the scaphoid fossa plus the area underlying the radioscaphocapitate ligament was regarded as the fixed proximal support. A fracture was produced at the scaphoid waist in all cases. The location of failure of bone at its anterior or dorsal cortex, either in tension or in compression, was determined by the site of application of the load. The anterior cortex failed in compression when the point of impact was located along the trapezium facet or the entire distal pole, whereas it failed in tension when the point of impact was along the trapezoid facet.

Keywords

Finite element analysis, fracture mechanism, humpback deformity, scaphoid fracture, scaphoid waist

Date received: 22nd August 2022; revised: 27th November 2022; accepted: 28th November 2022

Introduction

Most scaphoid fractures are of low energy type, resulting either from a sporting event or from a fall on an outstretched hand; the rest are of high energy type from falls from heights or motor vehicle accidents (Hackney and Dodds, 2011; Wolfe et al., 2016). The long axis of the scaphoid is oblique and is oriented within the carpus with an intra-scaphoid angle of 40° (SD 3°) in the coronal and 32° (SD 5°) in the sagittal plane (Heinzelmann et al., 2007). The unique anatomy of the scaphoid and the retrograde nature of its blood supply have implications for the nature of scaphoid fractures and their potential for healing (Hackney and Dodds, 2011). In adults, the risk for developing a scaphoid nonunion has been reported to be around 2% to 12% (Jørgsholm et al., 2020).

It has been suggested that in hyperextension of the wrist the proximal and distal poles of the scaphoid remain firmly attached to the bones of the respective carpal rows, making the scaphoid waist the fulcrum and thereby prone for a fracture (Slutsky and Slade, 2011). The radioscaphocapitate (RSC) ligament originates from the anteroradial aspect of the distal

radius, crosses the scaphoid and lies in the anterior concavity of its waist, or the middle third, proceeding distally and ulnarly to the capitate. The RSC ligament acts as a pivot for scaphoid rotation and, along with the taut palmar capsule, is thought to play a role in the mechanism of fracture when the wrist is loaded in hyperextension (when there is more than 95° of extension) and radial deviation (Clementson et al., 2020; Lee et al., 2012; Weber and Chao, 1978; Wolfe et al., 2016).

Although the waist is the most common anatomical location for a scaphoid fracture, the exact mechanism and the factors responsible for a fracture at

¹Department of Orthopaedics, All India Institute of Medical Sciences, Bhopal, Madhya Pradesh, India

²Department of Mechanical Engineering, Maulana Azad National Institute of Technology Bhopal, Madhya Pradesh, India

Corresponding Author:

John Ashutosh Santoshi, Department of Orthopaedics, All India Institute of Medical Sciences, Bhopal, Madhya Pradesh 462 020, India.

Email: jasantoshi@gmail.com

this particular location are still not completely understood (Clementson et al., 2020; Wolfe et al., 2016). Finite element analysis (FEA) is often considered to be an ideal method to simulate the mechanism of injury and study the formation of fractures in various bones (Herrera et al., 2012). In order to understand the mechanism of scaphoid waist fracture, we carried out a computational investigation to create a three-dimensional (3-D) Standard Tessellation Language (STL) format file and finite element (FE) model of the scaphoid using Digital Imaging and Communications in Medicine (DICOM) images. Using computer software, we then attempted to create and study the fracture formation in the FE model by applying forces approximately equivalent to those seen in common scenarios that result in scaphoid fractures.

Methods

Materials

Institutional Human Ethics Committee approval was obtained before the study (ref. IHEC-LOP/2021/IM0360). Clinical computed tomography (CT) scan of 12 uninjured wrists were used; these were of the contralateral wrist in cases of distal radial fractures or malunions, and of the ipsilateral wrist in scans reported 'normal', including two cases of pilon fracture of the middle phalanx. The images had been obtained in the 'wrist prone position' with slice width of 1 mm. The DICOM files obtained from the CT scans were used to construct STL models of the scaphoid. The scaphoid bone was defined using its geometry (computer-aided design [CAD] model) and material properties.

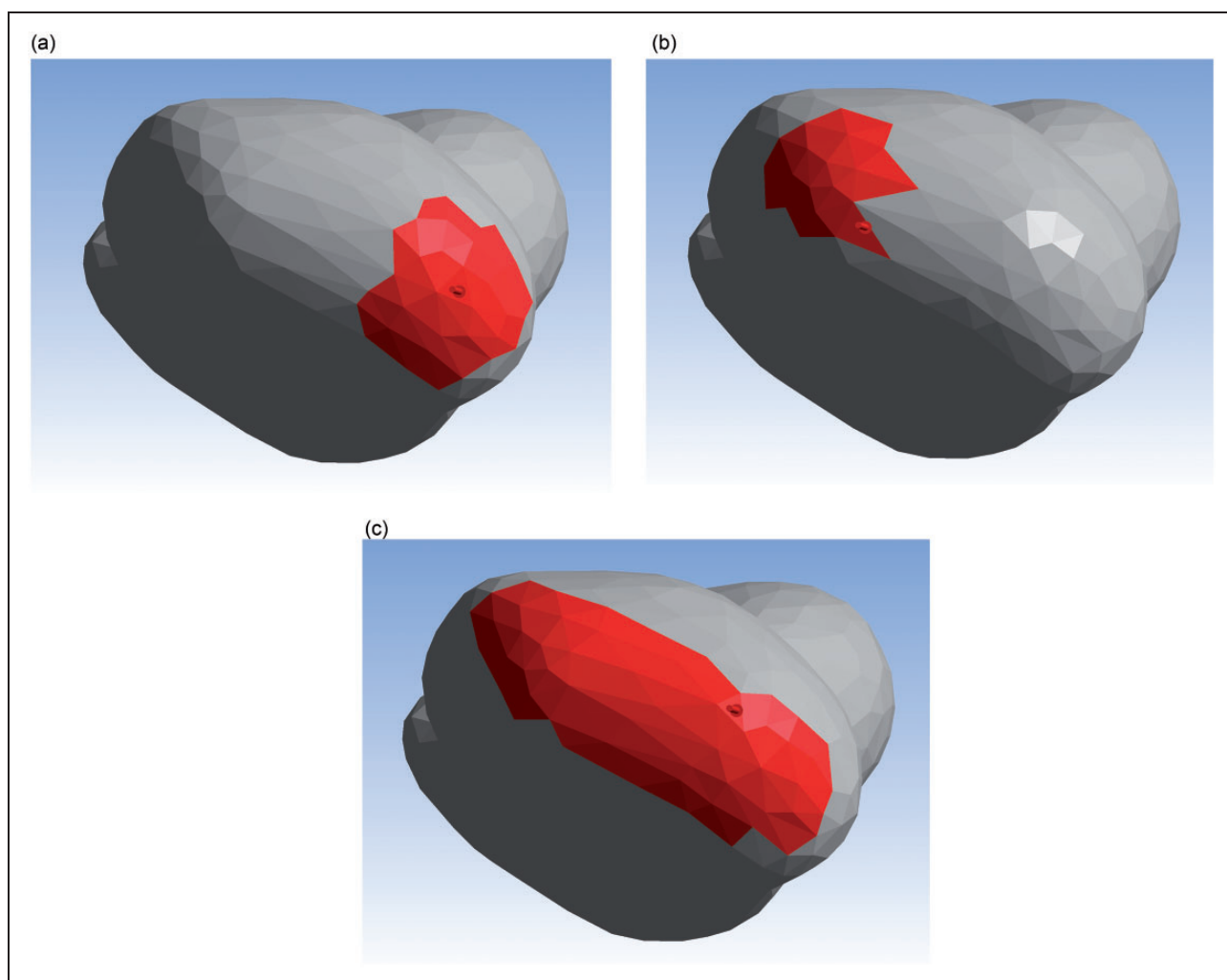


Figure 1. The point of loading at different sites along the scaphotrapeziotrapezoid (STT) joint as seen from the posterosuperior aspect of a computer-aided design model of the left scaphoid. (a) At the trapezium facet, (b) at the trapezoid facet and (c) along the entire STT joint. Images used courtesy of ANSYS, Inc.

The mechanism of injury was defined with loads and boundary conditions. With these defining parameters the FE analysis was carried out using ANSYS 2022 R1 Student (Ansys® Academic Research Mechanical).

Modelling of the scaphoid bone

The scaphoid STL models were further rectified and converted into a CAD model using Autodesk Meshmixer (RRID:SCR_015736, © 2020 Autodesk, Inc.) and FreeCAD (version 0.19.2), respectively.

Material properties

The material properties of the scaphoid, namely Young's modulus (10 GPa) and Poisson's ratio (0.3)

were extracted from the study of Bevers et al. (2021). Uniform material properties throughout the bone were used to define the behaviour of the scaphoid bones for performing the FEA.

Loads

While it is known that axial loading with hyperextension and radial deviation of the wrist is required to produce a scaphoid waist fracture, the exact amount of force required to produce this fracture is not known. We studied two common scenarios of low and high energy impacts in a forward fall on the hyperextended and radially deviated wrist for the FEA. We considered a peak impact force of 1.6 kN for the low energy scenario and of 4 kN for the high

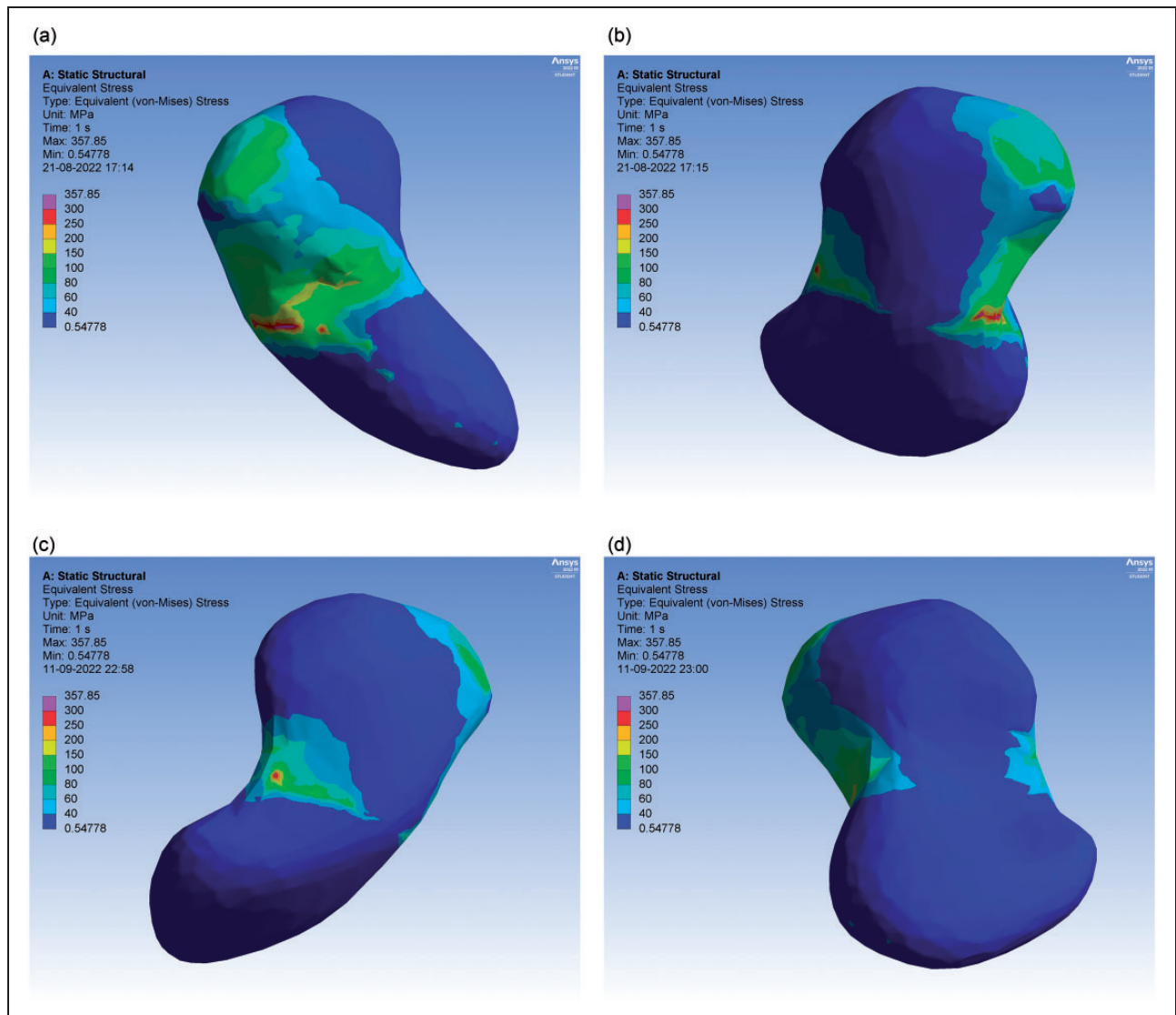


Figure 2. Finite element simulation of a load of 1.6 kN at the trapezium facet of the left scaphotrapeziotrapezoid joint. (a) View from the anterior aspect, (b) view from the radial aspect, (c) view from the posterior aspect and (d) view from the ulnar aspect. Images used courtesy of ANSYS, Inc.

energy scenario. For each scaphoid, the points of loading were at different sites along the scaphotrapezotrapezoid (STT) joint: radially at the trapezium facet, ulnarly at the trapezoid facet and along the entire STT joint. The scaphoid fossa plus the area underlying the RSC ligament were considered as the fixed proximal support. Figure 1 shows the sites of loading at the STT joint.

Results

The mean age of the 12 patients whose clinical CT scans were used for the study was 32 years [range 18

to 53]. There were four women and five scaphoids were from the right side. With a peak impact force of 1.6 kN, a fracture was produced at the scaphoid waist under a maximum von Mises stress of 464 MPa (SD 118), 285 MPa (SD 94) and 257 MPa (SD 110) when the loading was at the trapezium facet, the trapezoid facet and the entire STT joint, respectively (Figures 2 to 4). Similarly, with a peak impact force of 4.0 kN, a fracture was produced at the scaphoid waist under a maximum von Mises stress of 1161 MPa (SD 295), 712 MPa (SD 235) and 654 MPa (SD 289), respectively, as approximated in the FE analysis (Figures 5 to 7).

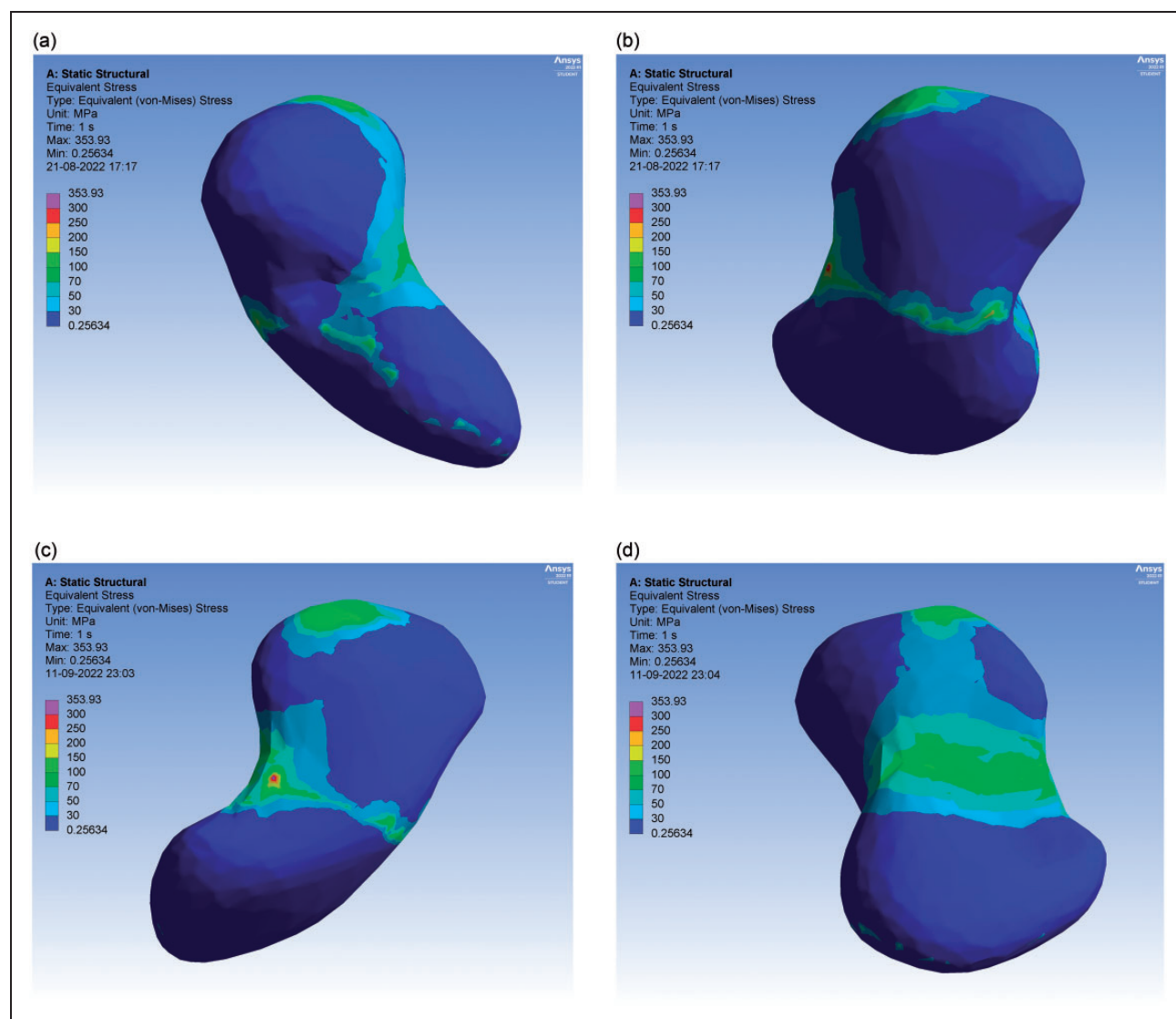


Figure 3. Finite element simulation of a load of 1.6 kN at the trapezoid facet of the left scaphotrapezotrapezoid joint. (a) View from the anterior aspect, (b) view from the radial aspect, (c) view from the posterior aspect and (d) view from the ulnar aspect. Images used courtesy of ANSYS, Inc.

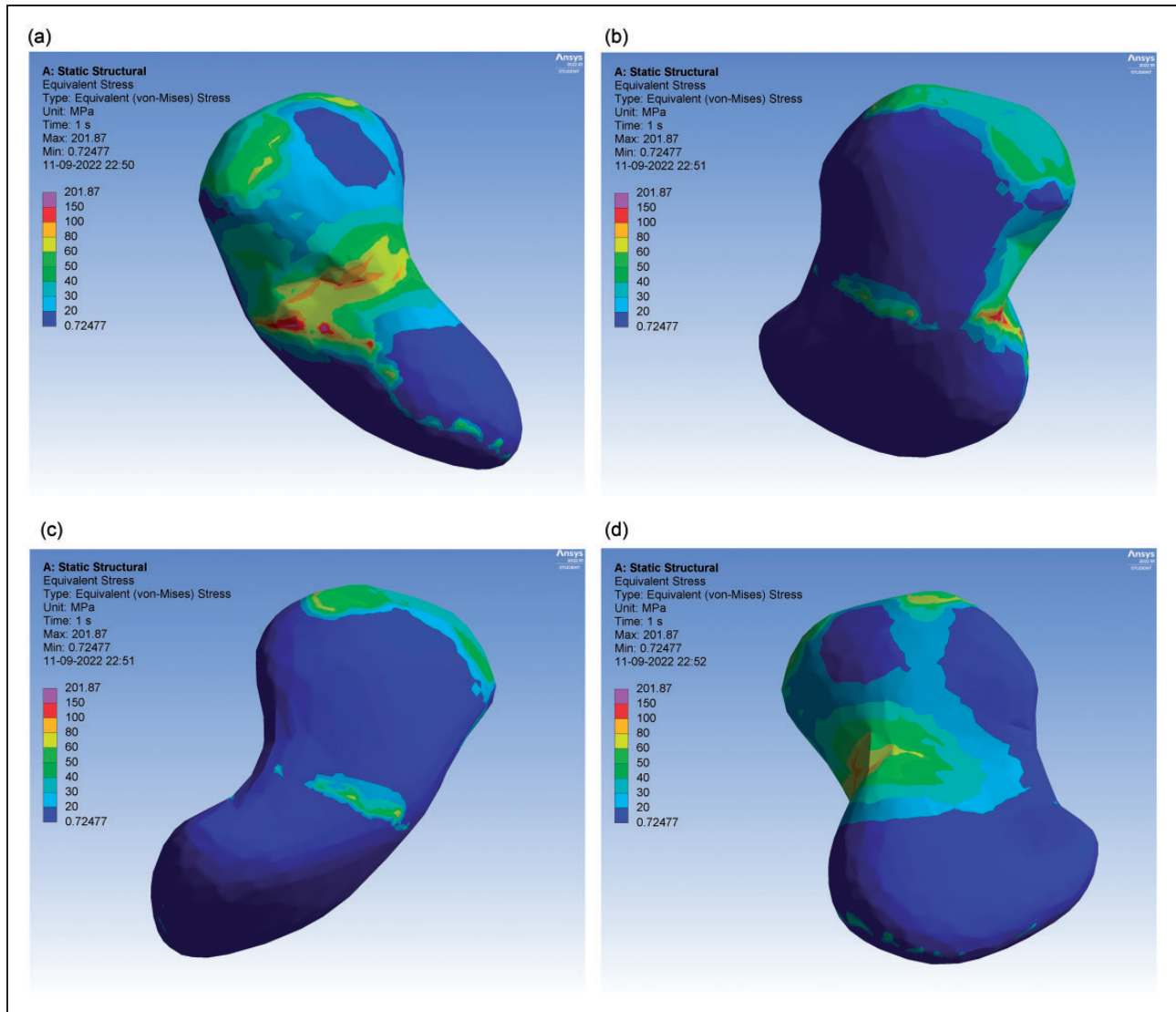


Figure 4. Finite element simulation of a load of 1.6 kN along the entire scaphotrapeziotrapezoid joint of the left scaphoid. (a) View from the anterior aspect, (b) view from the radial aspect, (c) view from the posterior aspect and (d) view from the ulnar aspect. Images used courtesy of ANSYS, Inc.

In both scenarios we obtained the primary fracture line at the scaphoid waist. The anterior cortex failed in compression when the point of impact was located radially, namely at the trapezium facet, and when the load was applied along the entire STT joint, whereas the anterior cortex failed in tension when the point of impact was located ulnarly, namely at the trapezoid facet.

Discussion

In the scenarios studied by us, the maximum von Mises stress, which indicates whether a given material will yield or fracture, was noted at the scaphoid waist, thereby corroborating it to be the most

common location of fracture when the scaphoid is loaded axially with the wrist in hyperextension and radial deviation.

For both impact loads, the von Mises stress was highest when the force was applied at the trapezium facet and least when the entire STT joint was loaded. Under the low energy impact force of 1.6 kN, the von Mises stress at the scaphoid waist was quite low compared with the high energy impact force of 4.0 kN. Thus, the low energy impact associated injury mechanism could result in an occult fracture or the stable acute type A2 fracture pattern, which is an incomplete crack fracture through the waist according to the Herbert and Fisher classification (Ten Berg et al., 2016). Such an injury may be misjudged by the patient

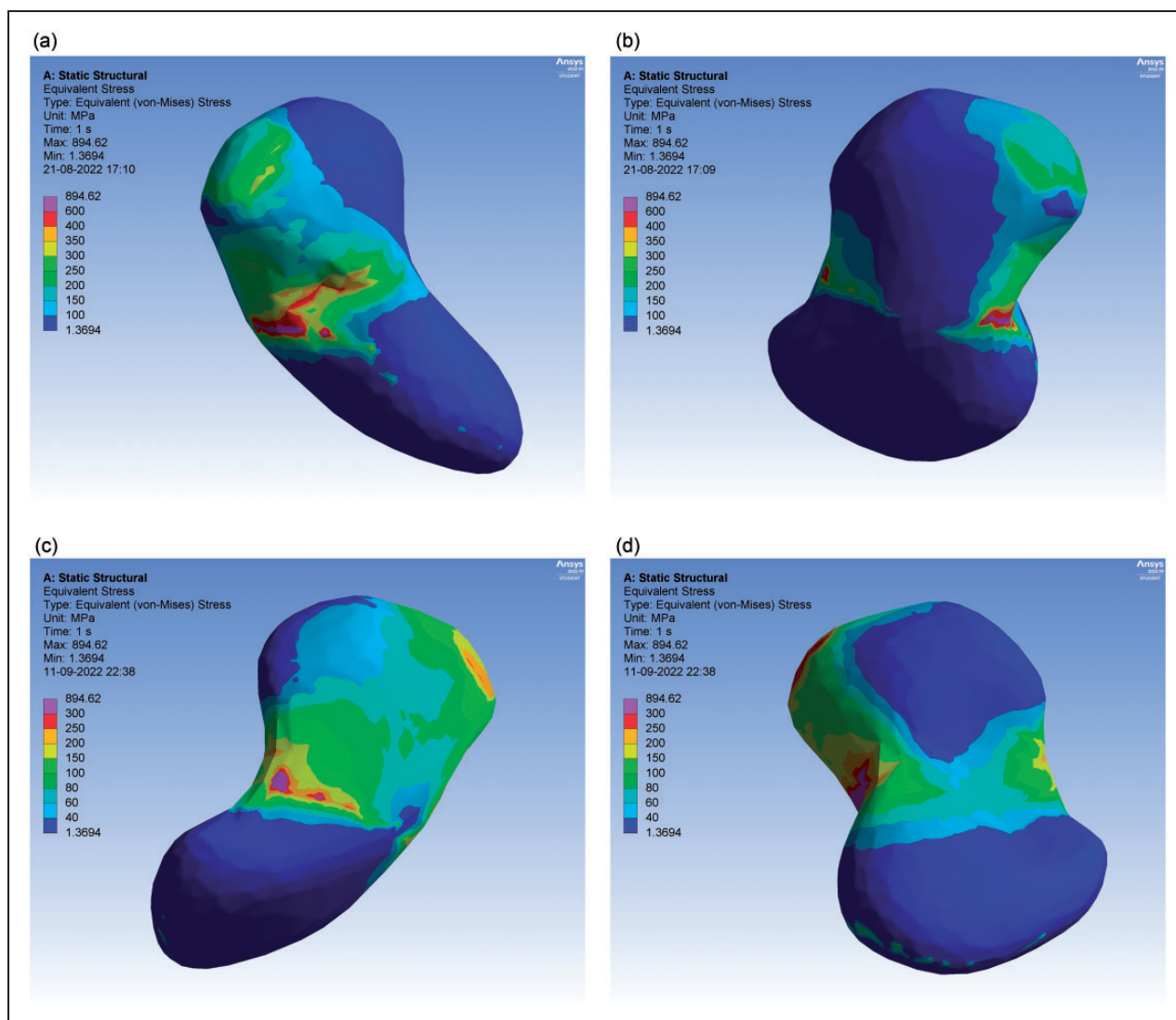


Figure 5. Finite element simulation of an axial load of 4 kN at the trapezium facet of the left scaphotrapeziotrapezoid joint. (a) View from the anterior aspect, (b) view from the radial aspect, (c) view from the posterior aspect and (d) view from the ulnar aspect. Images used courtesy of ANSYS, Inc.

and the treating physician as a wrist sprain and may present late as a scaphoid waist nonunion when the patient develops pain in the wrist secondary to the altered biomechanics and arthritis (Wolfe et al., 2016). Alternatively, it may unite with minimal or no immobilization, although reports of such cases are few (Adolfsson et al., 2020). In contrast, the high energy impact force could result in a complete and displaced fracture, which would be more easily identified on routine imaging studies of the wrist and therefore less likely to be missed. If missed, this injury could present late with a nonunion or a hump-back deformity of the scaphoid, or both.

The exact amount of force required to produce scaphoid waist fractures is not known. Weber and

Chao (1978) produced scaphoid waist fractures in their cadaveric experiments when wrists in 95° to 100° dorsiflexion with slight radial deviation were loaded with 460 to 960 pounds-force; these loads are ~2 kN and ~4.3 kN, respectively, and are roughly equal to the forces used in the present study (1.6 and 4.0 kN). In their study of force transmission through the wrist, Majima et al. (2008) found that when the wrist was loaded in the extended position, the scaphoid became vertically oriented, stabilized between the dorsal ridge of the radius and the anterior ligaments, and high pressure areas were concentrated on both its poles.

Most studies describing of mechanism of scaphoid fracture state that failure in compression occurs at

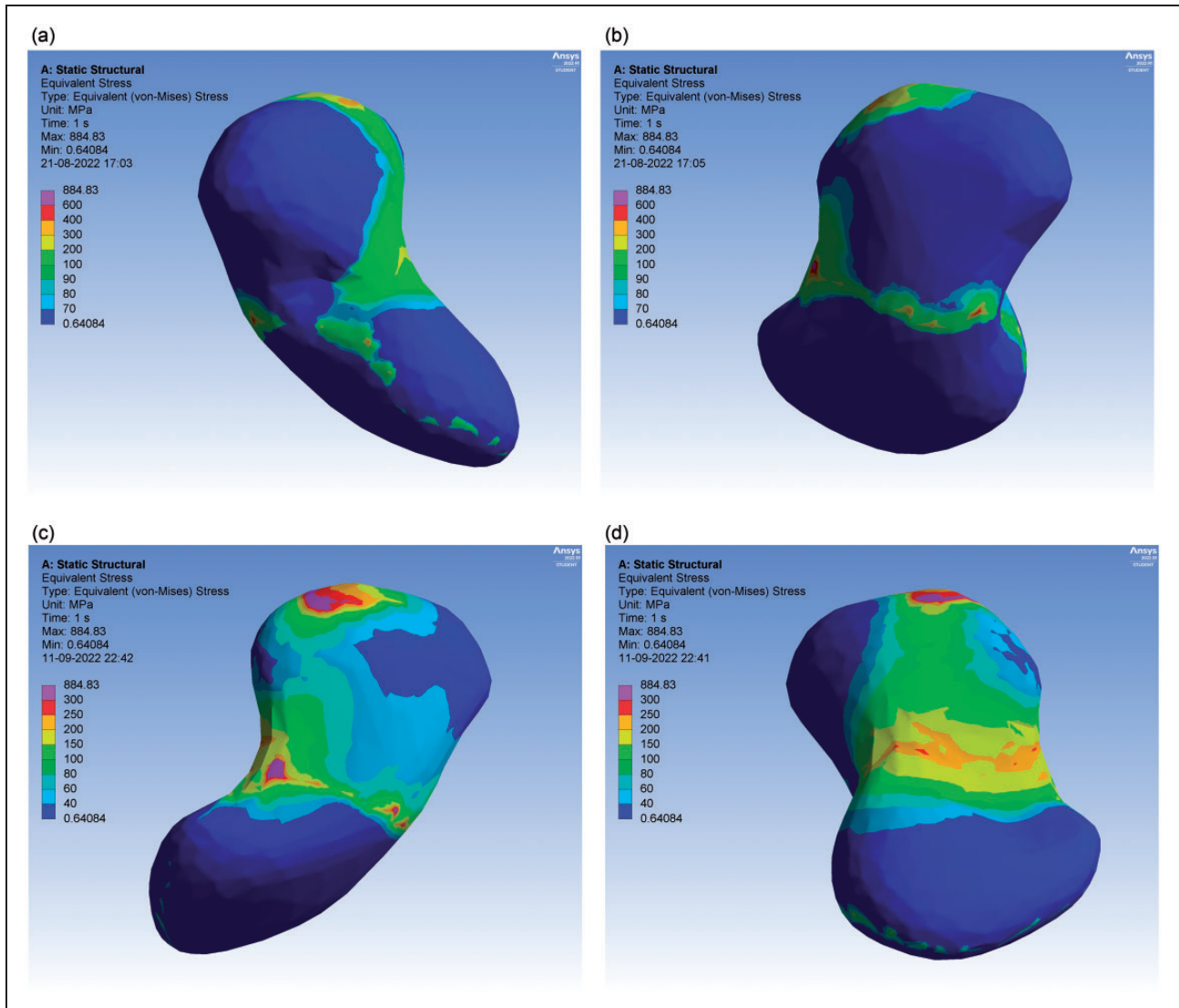


Figure 6. Finite element simulation of a load of 4 kN at the trapezoid facet of the left scaphotrapeziotrapezoid joint. (a) View from the anterior aspect, (b) view from the radial aspect, (c) view from the posterior aspect and (d) view from the ulnar aspect. Images used courtesy of ANSYS, Inc.

the dorsal cortex of the bone, whereas failure in tension occurs on the anterior cortex [Wolfe et al., 2016]; this is consistent with our finding when the load was applied ulnarly along the STT joint. When the load is applied radially or along the entire STT joint, the anterior cortex of the bone fails in compression (Figures 2, 4, 5 and 7); any consequent comminution at the anterior cortex, along with the natural tendency of scaphoid to flex, could be the precursor for the humpback deformity, which is frequently seen when there is a scaphoid malunion or nonunion.

Bone strength is determined by the bone geometry, cortical thickness and porosity, trabecular bone morphology and the intrinsic properties of bony tissue [Ammann and Rizzoli, 2003]. Bevers et al.

[2021] have reported that, in the scaphoid, the thickness of the cortical bone is approximately 1–1.5 times the thickness of the individual trabeculae and hence the two can be considered comparable. The microarchitecture of the scaphoid has been studied using microcomputed tomography (μ CT), which involves taking sections at 30 to 40 μ m; however, owing to the large amounts of radiation required, μ CT is suitable only for experimental studies. Using μ CT studies, it has been found that the scaphoid has a narrow rim of cortex enclosing dense trabecular bone and this trabecular pattern varies in the different regions within the bone and is found to follow the vascular distribution. The trabeculae are tightly packed within the two poles and run for only a

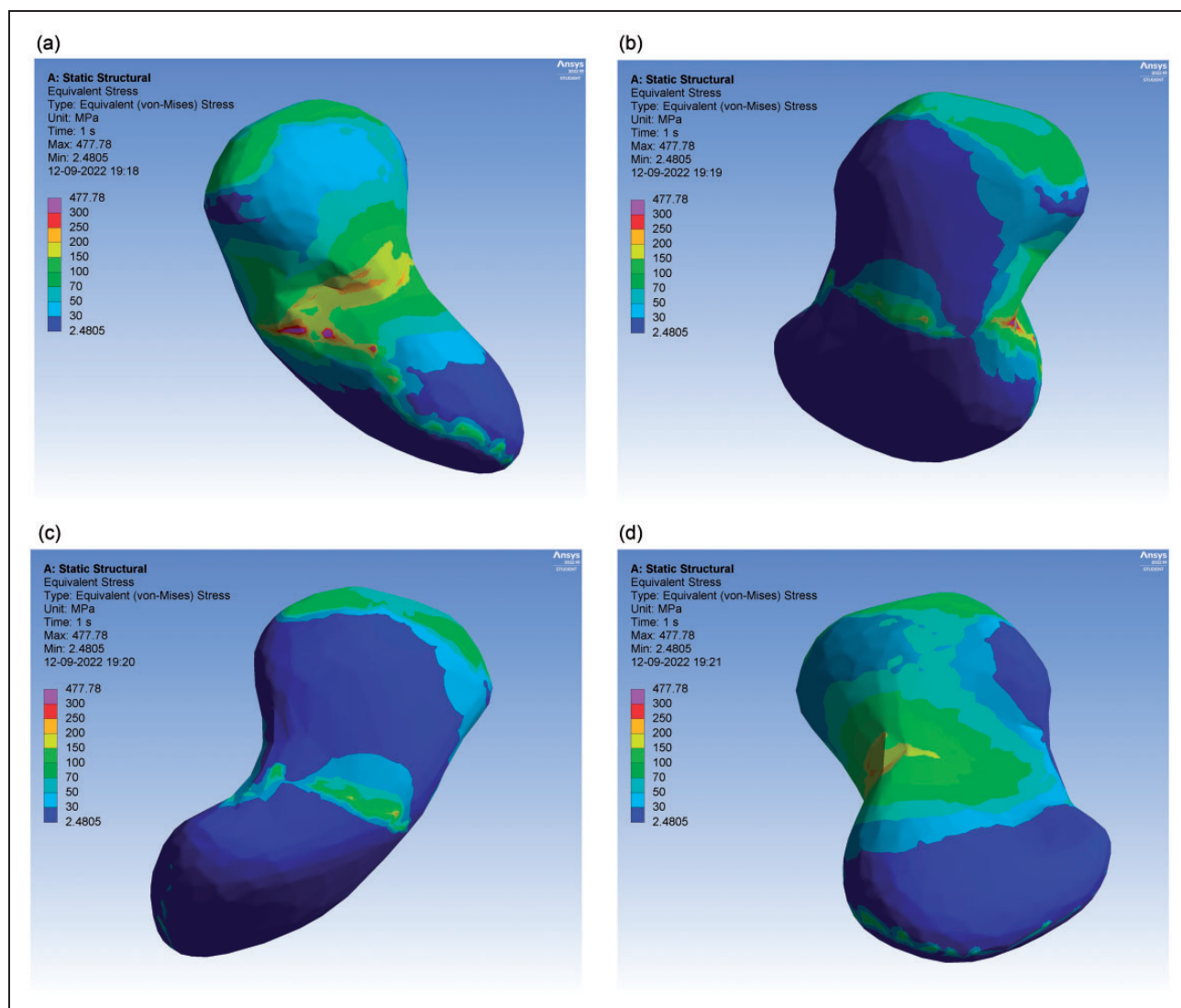


Figure 7. Finite element simulation of a load of 4 kN along the entire scaphotrapeziotrapezoid joint of the left scaphoid. (a) View from the anterior aspect, (b) view from the radial aspect, (c) view from the posterior aspect and (d) view from the ulnar aspect. Images used courtesy of ANSYS, Inc.

short distance. At the waist, the trabeculae are thin and sparsely arranged. This unique microarchitecture has been suggested to be the factor that makes the scaphoid waist the most common site for a fracture [Slutsky and Slade, 2011]. In the present study, like that of Bevers et al. (2021), uniform material properties were assigned throughout the bone thus making this a reproducible model for studying this injury mechanism; at the same time, we hypothesize that it is the unique morphology of the bone that has a major role in the formation of scaphoid waist fracture.

We attempted to study the scaphoid waist fracture formation in two common clinical scenarios, but we did not determine the ultimate stress at which the fracture

and displacement occurred. The use of clinical CT scans precluded the determination of the role of cartilage thickness in fracture formation, which may have affected the results of FEA. However bones have elastic properties that are several orders of magnitude higher than those of soft tissues, and are often assumed to be rigid bodies [Varga et al., 2013], so the role of cartilage thickness in fracture formation could be minimal.

Despite these limitations, we have analysed a representative sample of young individuals in whom scaphoid waist fractures are commonly seen. On axial loading with the wrist in hyperextension and radial deviation, the scaphoid fracture occurs at the waist, as is seen commonly in clinical practice. However, the location of failure of bone at its anterior


or dorsal cortex, in tension or in compression, is determined by the site of application of load at the STT joint. The humpback deformity, seen in scaphoid malunion or nonunion, is probably a consequence of a fracture from high energy loading along the trapezium facet or the entire STT joint, compounded by the natural tendency of scaphoid to flex.

Declaration of conflicting interests The authors declare no potential conflicts of interest with respect to the research, authorship, and/or publication of this article.

Funding The authors received no financial support for the research, authorship, and/or publication of this article.

Informed consent Waiver of consent was requested from the Ethics committee as anonymized patient data (computed tomography scans) was used for the study. There is no information (names, initials, hospital identification numbers or photographs) in the submitted manuscript that can be used to identify patients.

Ethical approval Obtained from Institutional Human Ethics Committee of the All India Institute of Medical Sciences, Bhopal, MP, India, on 4 May 2021. Approval no. IHEC-LOP/2021/IM0360.

ORCID iD John Ashutosh Santoshi  <https://orcid.org/0000-0002-2149-7525>

References

- Adolfsson L, Hallgren HB, Tegner Y. Union of scaphoid waist fractures in adults despite no or minimal immobilization – a report of five cases. *SN Compr Clin Med*. 2020; 2: 491–5.
- Ammann P, Rizzoli R. Bone strength and its determinants. *Osteoporos Int*. 2003; 14: S13–8.
- Beyers MSAM, Daniels AM, van Rietbergen B et al. Assessment of the healing of conservatively-treated scaphoid fractures using HR-pQCT. *Bone*. 2021; 153: 116161.
- Clementson M, Björkman A, Thomsen NOB. Acute scaphoid fractures: guidelines for diagnosis and treatment. *EFORT Open Rev*. 2020; 5: 96–103.
- Hackney LA, Dodds SD. Assessment of scaphoid fracture healing. *Curr Rev Musculoskelet Med*. 2011; 4: 16–22.
- Heinzelmann AD, Archer G, Bindra RR. Anthropometry of the human scaphoid. *J Hand Surg Am*. 2007; 32: 1005–8.
- Herrera A, Ibarz E, Cegoñino J et al. Applications of finite element simulation in orthopedic and trauma surgery. *World J Orthop*. 2012; 3: 25–41.
- Jørgsholm P, Ossowski D, Thomsen N, Björkman A. Epidemiology of scaphoid fractures and non-unions: a systematic review. *Handchir Mikrochir Plast Chir*. 2020; 52: 374–81.
- Lee SB, Kim HJ, Chun JM et al. Osseous microarchitecture of the scaphoid: cadaveric study of regional variations and clinical implications. *Clin Anat*. 2012; 25: 203–11.
- Majima M, Horii E, Matsuki H, Hirata H, Genda E. Load transmission through the wrist in the extended position. *J Hand Surg Am*. 2008; 33: 182–8.
- Slutsky DJ, JF Slade (Eds.). *The scaphoid*. Stuttgart, Georg Thieme Verlag, 2011.
- Ten Berg PW, Drikkoningen T, Strackee SD, Buijze GA. Classifications of acute scaphoid fractures: a systematic literature review. *J Wrist Surg*. 2016; 5: 152–9.
- Varga P, Schefzig P, Unger E, Mayr W, Zysset PK, Erhart J. Finite element based estimation of contact areas and pressures of the human scaphoid in various functional positions of the hand. *J Biomech*. 2013; 46: 984–90.
- Weber ER, Chao EY. An experimental approach to the mechanism of scaphoid waist fractures. *J Hand Surg Am*. 1978; 3: 142–8.
- Wolfe SW, Pederson WC, Hotchkiss RN, Kozin SH, Cohen MS. *Green's operative hand surgery*, 7th Edn. Philadelphia, Elsevier Health Sciences, 2016: 588–624.